

Light from the Cosmic Frontier: Gamma-Ray Bursts

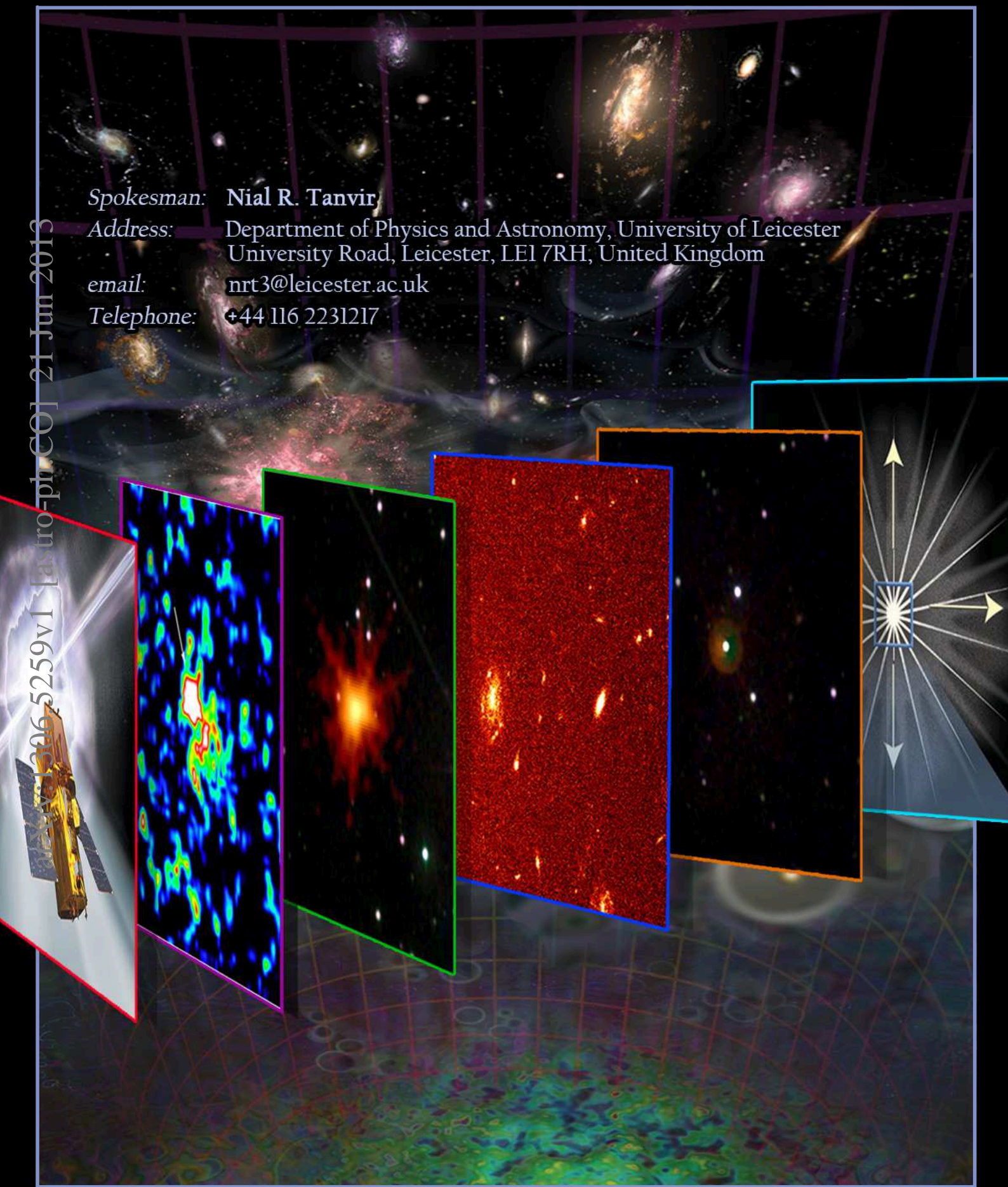
Spokesman: **Nial R. Tanvir**

Address: Department of Physics and Astronomy, University of Leicester
University Road, Leicester, LE1 7RH, United Kingdom

email: nrt3@leicester.ac.uk

Telephone: +44 116 2231217

arXiv:1306.5259v1 [astro-ph.CO] 21 Jun 2013



Authors:

L. Amati (INAF/IASF Bologna), J.-L. Atteia (IRAP/CNRS/UPS Toulouse),
L. Balazs (Konkoly Obs.), S. Basa (LAM Marseille), J. Becker Tjus (Univ. Bochum),
D.F. Bersier (Liverpool Univ.), M. Boër (CNRS-ARTEMIS Nice), S. Campana (INAF/OAB Brera),
B. Ciardi (MPA Garching), S. Covino (INAF/OAB Brera), F. Daigne (IAP Paris),
M. Feroci (INAF/IAPS Rome), A. Ferrara (SNS Pisa), F. Frontera (INFN/Univ. Ferrara),
J.P.U. Fynbo (DARK Copenhagen), G. Ghirlanda (INAF/OAB Brera),
G. Ghisellini (INAF/OAB Brera), S. Glover (Uni. Heidelberg), J. Greiner (MPE Garching),
D. Götz (CEA Saclay), L. Hanlon (UCD Dublin), J. Hjorth (DARK Copenhagen),
R. Hudec (AI AS CR Ondřejov & CTU Prague), U. Katz (Univ. Erlangen),
S. Khochfar (Univ. Edinburgh), R. Klessen (Univ. Heidelberg), M. Kowalski (Univ. Bonn),
A.J. Levan (Univ. Warwick), S. McBreen (UCD Dublin), A. Mesinger (SNS Pisa),
R. Mochkovitch (IAP Paris), P. O'Brien (Univ. Leicester), J.P. Osborne (Univ. Leicester),
P. Petitjean (IAP Paris), O. Reimer (Univ. Innsbruck), E. Resconi (TU München),
S. Rosswog (Univ. Stockholm), F. Ryde (KTH Stockholm), R. Salvaterra (INAF/IASF Milano),
S. Savaglio (MPE Garching), R. Schneider (INAF/Oss. Rome), G. Tagliaferri (INAF/OAB Brera),
A. van der Horst (Univ. Amsterdam)

Supporters:

M. Ackermann (DESY Zeuthen), Z. Bagoly (Eötvös Univ.), E. Bernardini (DESY Zeuthen),
J.H. Black (Chalmers Univ. of Techn.), P. Clark (Uni. Heidelberg), B. Cordier (CEA Saclay),
J.-G. Cuby (LAM Marseille), F. Ferrini (Univ. Pisa), C. Finley (Stockholm Univ.),
S. Klose (Tautenburg Obs.), A. Klotz (IRAP/CNRS/UPS Toulouse),
T. Krühler (DARK Copenhagen), N. Langer (Univ. Bonn), K. Mannheim (Würzburg Univ.),
E. Nakar (Wise Obs.), C.-N. Man (ARTEMIS, CNRS/OCA Nice),
M. Pohl (DESY Zeuthen, Potsdam Univ.), P. Schady (MPE Garching), S. Schanne (CEA Saclay),
V. Springel (ITS Heidelberg), P. Sutton (Cardiff Univ.), N. van Eijndhoven (Brussel Univ.),
J.-Y. Vinet (ARTEMIS, CNRS/OCA Nice), A. Vlasis (CPA Leuven),
D. Watson (DARK Copenhagen), K. Wiersema (Univ. Leicester)

Supporters from non-ESA member states:

V. Bromm (Univ. Texas Austin), N. Gehrels (GSFC), N. Kawai (Tokyo Inst. Techn.)

1 Executive Summary

Gamma-Ray Bursts (GRBs) are the most powerful cosmic explosions since the Big Bang, and thus act as signposts throughout the distant Universe. Over the last 2 decades, these ultra-luminous cosmological explosions have been transformed from a mere curiosity to essential tools for the study of high-redshift stars and galaxies, early structure formation and the evolution of chemical elements. In the future, GRBs will likely provide a powerful probe of the epoch of reionisation of the Universe, constrain the properties of the first generation of stars (Fig. 1), and play an important role in the revolution of multi-messenger astronomy by associating neutrinos or gravitational wave (GW) signals with GRBs.

Here, we describe the next steps needed to advance the GRB field, as well as the potential of GRBs for studying the Early Universe and their role in the upcoming multi-messenger revolution. We identify the following fundamental questions as the prime science drivers for the next two decades:

- When did the first stars form, what are their properties, and how do Pop III stars differ from later star formation in the presence of metals?
- When and how fast was the Universe enriched with metals?
- How were the first structures formed which then developed into the first galaxies?
- How did reionisation proceed as a function of environment, and was radiation from massive stars its primary driver?
- What is the relation between GRB rate and star formation rate, and what is its evolution with time? What is the true redshift distribution and corresponding luminosity function of long GRBs?
- How are γ -ray and neutrino flux in GRBs related, and how do neutrinos from long GRBs constrain the progenitor and core-collapse models?
- Can short-duration GRBs be unambiguously linked to gravitational wave signals, and what do they tell us about the neutron star merger scenario?
- What are the electromagnetic counterparts to gravitational waves and neutrino bursts?

These questions relate directly to the Cosmic Vision theme #4, “*How did the Universe originate and what is it made of?*”, in particular to 3 out of the 8 goals: **(1) Find the first gravitationally-bound structures that were assembled in the Universe – precursors to today’s galaxies and cluster of galaxies – and trace their evolution to the present.** Since GRBs can be detected from extreme distances ($z \sim 30\text{--}60$ [2]), accurate localisations provide the best-possible pointers to the first stars, and to the proto-galaxies where they form. This will find the first black holes (BH), likely to be the seeds of the supermassive BHs which dominate the X-ray luminosity of the current Universe.

GRBs in Cosmological Context

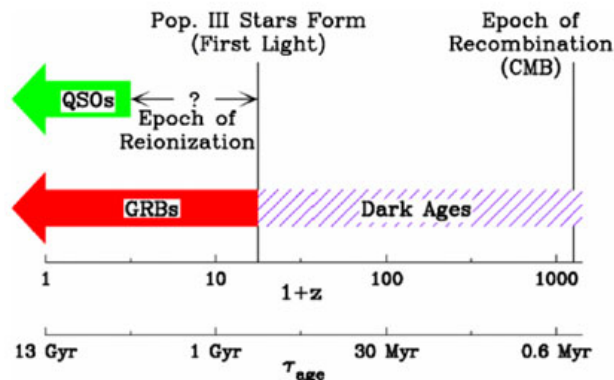


Figure 1: GRBs in the cosmological context. (From [1])

(2) ...Trace the life cycle of chemical elements through cosmic history. Since long GRBs are produced by massive stars [3], which have short life-times, the GRB rate traces the star formation (SF) rate. The extraordinary brightness and minimised absorption bias make GRBs particularly useful SF indicators. Optical/NIR afterglow spectroscopy allows to measure line-of-sight metallicity at exquisite detail, and map the cosmic chemical evolution with high- z GRBs. Short GRBs are likely linked to the formation of the heaviest elements in the Universe, such as platinum.

(3) ...Examine the accretion processes of matter falling into black holes..., and look for clues to the processes at work in gamma-ray bursts. The prompt γ /X-ray emission of GRBs, combined with polarisation measurements provides direct clues on the accretion and jet ejection processes. Optical/NIR absorption line diagnostics will link this to progenitor properties, thus allowing us to understand the basic picture of GRB-production.

To fully utilise GRBs as probes of the early Universe and/or as multi-messengers requires (i) a detection system for 5000 GRBs, among them 50 GRBs at $z > 10$, (ii) a means to localise them quickly and accurately, (iii) instrumentation to determine their redshift quickly, preferentially on the fly, and (iv) low-latency communication to the ground.

Instead of proposing a single strawman mission concept, we describe the instrumentation needed to answer each of the above fundamental questions, and describe options how to realise the measurements depending on the priorities among those questions.

The authors of this WP agree in the choice of emphasising the role GRBs can and will play in the study of the high-redshift Universe, but also recognise the huge potential of GRBs for the coincident detection of GW or neutrinos and electromagnetic signals [4]. It may confirm the basic model of the short GRBs, finally clarify the origin of the heaviest elements, and allow for a precise measurement of the expansion rate of the Universe.

2 The astrophysics landscape until 2030

The landscape of astronomy 15-20 years from now will be dominated by a wealth of new facilities across the entire electromagnetic (EM) spectrum and beyond, as non-photonic sources open a previously inaccessible window into many of the most extreme regions of the Universe. It is against this landscape that new space missions and ground-based facilities must be measured and judged. While any attempt to prescribe precisely the likely scientific frontiers at this time is fraught with uncertainty, a variety of possibilities bear consideration. We outline a range of facilities that may be operational in this time scale, along with their contribution to the science questions. A GRB-focussed mission would provide a huge step in our understanding of the early Universe, impossible by any of the facilities in the planning, and at the same time would enable some of these planned facilities to perform science that would be otherwise impossible. GRBs are the most luminous sources on the sky, releasing in less than a minute the energy output of the Sun over its entire life. Several GRBs occur each day, and thus GRBs act as frequently available signposts throughout the Universe. Two sub-groups of GRBs are distinguished according to their duration (Fig. 2): (i) Long-duration GRBs (>2 s) are firmly linked to the collapse of massive stars, thus probing sites of star formation with little delay, as the star's lifetimes are measured in megayears and not gigayears. GRBs have been seen up to the highest measured redshifts. (ii) Short-duration GRBs likely originate from the merging of compact stars and are expected to produce strong gravitational waves. Both types of GRBs are powerful neutrino sources. As stellar sized objects at cosmological scales, they connect different branches of research and thus have a broad impact on present-day astrophysics.

2.1 High-Energy satellites

Over the next few years, progress on GRBs is likely to remain driven by the *Swift* mission. Its launch heralded an unprecedented period of progress towards GRB progenitors, as well as highlighting the varied and diverse high-energy sky in ways that were unanticipated prior to its launch. *Swift* achieved this due to a combination of a broad compliment of instruments dedicated to GRB detection and follow-up, and the implementation of a novel autonomous rapidly-slewing spacecraft. It has found the first GRBs at $z > 6, 7, 8$ and 9 , pinpointed the locations of short-GRB afterglows, identified nearby GRBs with and (importantly) without supernovae. Despite its 8 yr in orbit, it continues to discover new populations of high-energy transients in previously unexplored parameter space. *Swift* was joined in 2008 by the *Fermi* Gamma-ray Telescope – a powerful satellite with an unparalleled spectral range, opening new insights into

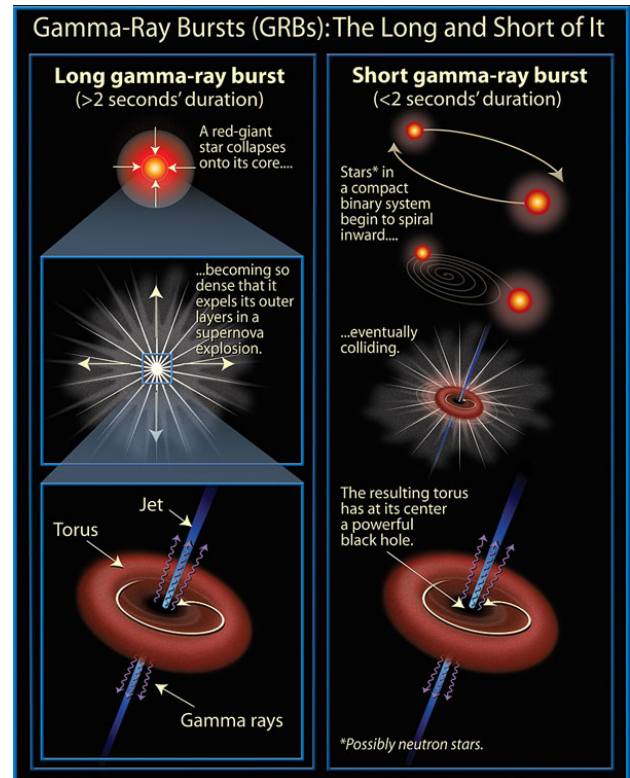


Figure 2: Long-duration GRBs (left) are thought to originate in the collapse of massive stars, while short-duration GRBs are likely produced in the merger of two compact objects. Both scenarios result in a relativistic jet which is responsible for producing the γ -ray emission. (From [5])

the nature of the γ -ray emission from GRBs, and enabling sensitive tests of differing models for quantum gravity. Real-time GRB detections are also provided by *INTEGRAL*, *AGILE*, *Suzaku*, *MAXI/ISS* and the interplanetary network (IPN) satellites.

These missions are all working well at present, but have finite lifetimes, governed both by orbital decay, instrument lifetime and, perhaps more importantly, financial constraints. It is unlikely that any of them will still be in operation well into the 2020s. Our window onto the transient high-energy sky thus revolves around new initiatives. Those likely in the interim period until 2028 are specialised instruments, often with lower sensitivity than *Swift* which will focus on individual science questions.

Four larger scale missions are the approved Indian *Astrosat*, the Japanese *Astro-H*, and the German/Russian *SRG*, as well as the planned French/Chinese *SVOM*. *Astrosat* is a multi-wavelength observatory covering the UV to hard X-ray bands scheduled for launch within a year, and may be expected to detect of order a dozen GRBs per year with its Scanning Sky Monitor. *Astro-H* is scheduled for launch in 2015, and might be able to obtain high-resolution spectra of GRB afterglows if target-of-opportunity observations can be rapidly scheduled. *SRG* will perform a sensitive all-

sky survey in the 0.3–12 keV band with the *eROSITA* and ART-XC telescopes, starting in 2015. In particular, *eROSITA* [6] with its good sensitivity is expected to detect 4–8 GRB afterglows per year [7], over a mission lifetime of at least 4 years. *SVOM* in many ways is modelled on the remarkable success of *Swift*, carrying γ -ray, X-ray and optical telescopes. The softer response (triggering at lower energy) and larger, red optimised optical telescope may enhance the recovery fraction for high- z GRBs.

Other future high-energy missions remain at an earlier stage of development, although there are plans in progress to launch small to moderate size detectors either as stand-alone missions or via the ISS. *LOFT* is currently under consideration for ESA's M3 launch slot as primarily a timing experiment, providing spectral sensitivity and timing resolution much better than *RXTE*. Its wide-field monitors make it a capable GRB detector. However, it has no automated slewing capability. In a 4 year mission it will see only < 2 GRBs at $z > 8$, even under optimistic assumptions [8]. Japan is planning an upgrade of *MAXI* on the ISS within the next few years, and NASA has recently accepted *NICER* [9], an X-ray timing and spectroscopy experiment for the ISS, with a launch date in 2017 which potentially could be used for GRB afterglow observations. The Russian space agency is planning for a small GRB mission within the next year with *UFFO*-pathfinder, a rapid detection system for prompt optical emission which later might evolve into a larger *UFFO* mission [10]. Planned for launch in the next years on the Chinese Tiangong-2 is a hard X-ray polarimeter for the study of GRBs, though this relies on the localisation and spectral measurements by a different satellite.

2.2 Multi-wavelength & multi-messenger domain

Outside of the high energy arena, the next years should see the long awaited start of routine multi-messenger astronomy, for which neutrinos from SN 1987A offered the first hints. The power of this non-photonic messenger, and gravitational waves as well, is to probe into highly enshrouded environments, invisible to electromagnetic observers. Both messengers are currently the subject of major investments, still have to reach a positive detection of signals from GRBs, but are expected to remedy this situation in the next decade.

Firstly, the upgrades to the *LIGO* and *VIRGO* interferometers will reach the point at which routine astrophysical detections of gravitational waves become reality [11]. This point should be reached towards the end of this decade [12]. Further away is a next generation of GW interferometer known as the Einstein Telescope (ET) [13] with a target operational date in the mid-2020's. Since these detectors measure gravitational wave strain, the observational horizon scales linearly with the sensitivity (unlike the inverse square

law for electromagnetic detectors). ET will be capable of seeing compact binary mergers to $z \sim 3$ (compared to the $z \sim 0.1$ for the next generation detectors). It will provide detection rates of 10^4 (10^5) for binary BH (NS) mergers [14], enabling detailed population and evolution studies. Mergers also provide a precise gravitational wave luminosity distance, giving a powerful probe of cosmology that can independently measure H_0 , Ω_M , Ω_Λ , w and \dot{w} . However, positional accuracy will be poor, even for ET operating in conjunction with further upgraded *ALIGO/AVIRGO* detectors. An EM trigger-system will therefore be needed to pinpoint source locations to an accuracy that allows measuring their redshifts, since it is the comparison of the redshift to the GW-determined distance that enables cosmological studies.

Secondly, IceCube, the largest neutrino telescope built so far, has been in operation since two years. First studies now reach beyond the level of predicted neutrino fluxes, but yielded no detection of GRB neutrinos so far [15]. The recently announced first hint of an astrophysical signal seen by IceCube provides great prospects for the identification of cosmic ray sources [16]. Possible reasons could be the choice of parameters for the standard neutrino flux calculations, in particular the Lorentz factor of the source, and the relation between accelerated electrons and protons. A more detailed treatment of the microphysics leads to a reduction of the general flux at fixed parameters, but does not take into account the general assumption that GRBs are the sources of ultra-high energy cosmic rays (UHECRs) [17]. Further studies will have to show if there is any significant spatial or temporal clustering that could be connected to GRBs and will help to study GRBs as possible cosmic ray sources. The future European neutrino telescope KM3NeT, to be deployed within this decade in the Mediterranean Sea, should provide another sensitivity boost, so that expectations remain high.

The end of this decade (or the start of the next) will see the advent of the James Webb Space Telescope (JWST) and large ground-based optical telescopes (ELT's). These are observatories rather than dedicated missions, with a science remit from exo-planets to cosmology. Central to the science case for each is the study of the early Universe. These large telescopes will be used to pin-point some of the most distant galaxies yet observed as well as providing spectroscopic capability beyond the limit of HST photometry. Nonetheless, even with these next generation facilities, spectroscopic studies remain challenging. If the faint end slope of the galaxy luminosity function is genuinely very steep [18, 19] then even these facilities will not probe it far down. If the first stars form in relatively faint and low mass haloes, it is quite likely that they will not be found directly by either facility, even in their deepest fields [20]. As we will describe later, GRBs offer a route around this prob-

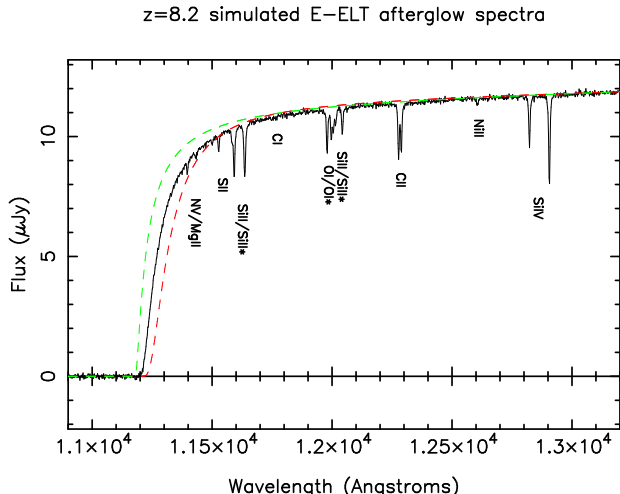


Figure 3: Simulated spectrum (solid line) around the Ly- α break showing the quality of data which would be obtained with a 30–40 m telescope such as the proposed E-ELT for an afterglow with magnitude approximately the same as that obtained for GRB 090423 (as observed by the VLT). The host galaxy was chosen to have an HI column density of 10^{21} cm^{-2} and a metallicity of $1/10 Z_{\odot}$, and the IGM to be 100% neutral. The green dashed line shows a model with just a neutral IGM (with redshift fixed at that given by the host metal lines). High S/N data can be used to decompose IGM and host galaxy contributions (red dashed line), thus determining each with good precision. This simulation also shows the excellent measurements of metal abundances that could be achieved with such observations.

lem. The 30–40 m telescopes will be able to provide unique information on the chemical enrichment and re-ionization history *if* they can be fed with accurate locations of high- z GRB afterglows (see Fig. 3 for a simulated E-ELT/HARMONI spectrum).

This period will also mark the launch of ESA’s GAIA and Euclid satellites. GAIA is primarily an astrometry mission, but due to the temporal sequence of its sky scans it will detect a large number of transients, among those up to 40 GRB afterglows [21, 22]. Euclid is predominantly aimed at providing precision measurements of cosmological parameters via weak lensing and baryon acoustic oscillations. The deep survey should reach optical/NIR magnitudes of $VYJH \sim 24$ over half of the sky by 2027, and may turn up a reasonable fraction ($\sim 30\%$) of low-redshift GRB hosts.

The Large Synoptic Survey Telescope (LSST) is due to start operation around 2022. It will locate of order 10^6 transients per night. High-energy coverage of a good fraction of these transients would be of significant interest to the community providing distinction between orphan GRB afterglows, tidal disruption flares, extreme supernovae, radioactively powered transients from GW sources and other yet unimagined transients. While LSST is expected to discover 4 GRB afterglows per night [21], it will be limited to $z < 7$ due to its filter set.

There are also significant ground-based investments across the electromagnetic spectrum, from the high frequency of the Cherenkov Telescope Array (CTA) to the low frequency radio arrays associated with the Square Kilometer Array (SKA). CTA will be sensitive to the highest energy γ -rays (> 10 TeV in some cases), and will probe high-energy emission from GRBs and their shocks in the first minutes after the bursts. The properties of the bursts at such high energy remain poorly understood at present, although the recent GRB 130427A was detected up to 120 GeV (rest-frame; [23]). Assuming the spectral-temporal extrapolations from presently detected GRBs by Fermi-LAT, CTA might detect just a few GRB/yr [24], but its orders-of-magnitude better sensitivity on short timescales compared to Fermi-LAT in the overlapping energy regime will provide a vast amount of photon data allowing to sensitively probe spectral-temporal evolution of GRBs at the upper end of the accessible electromagnetic spectrum. This will provide a handle on the prompt emission properties, and will be a powerful complement to our proposed mission – importantly, CTA will have a narrow field of view, and so will require triggers in order to re-point at GRBs. CTA should be operational towards the end of the decade. We may gain a somewhat earlier insight of the high-energy properties of GRBs via HAWC (the High Altitude Water Cherenkov Gamma-Ray observatory), which is already partially operational, and has the ability to trigger on > 1 TeV γ -ray photons across 15% of the sky, (though it lacks the sensitivity of CTA and its effective area decreases rapidly away from zenith).

Moving to longer wavelengths, the Atacama Large Millimeter Array (ALMA) will continue to be a workhorse instrument for astronomy, and its unique sensitivity to warm and cool dust in distance galaxies provides a means of probing the nature of the earliest galaxies, in particular of the highest redshift GRB hosts detected. In addition, ALMA will allow us to map systematically the GRB afterglow emission near its spectral peak, thus providing beaming-independent energy estimates. Finally, SKA, which should be operational with a partial array around 2020, will provide new insights into the formation of the first structures in the Universe and the re-ionisation through mapping the 21 cm line emission at different epochs. In the GRB field, SKA as well as its predecessors LOFAR, MWA and PAPER will be powerful facilities to study the radio afterglow emission, and will provide unique insights into the physics and environment properties of these sources. We expect that SKA will be sensitive enough to detect all afterglows of GRBs of a next generation γ -ray detector, and for 50% of those, will allow the estimate of their true (collimation corrected) energetics through late time (> 100 days) radio calorimetry [25].

3 Open Questions

3.1 GRBs and the Early Universe

3.1.1 GRB observability

The identification of very high redshift ($z > 7$) sources is challenging due to their great luminosity distances, and the difficulties of observing in the near-IR (NIR) from the ground. This is exacerbated by the effects of hierarchical structure growth, which means that galaxies start out increasingly small and faint intrinsically, and that bright quasars are exceptionally rare at $z > 7$. The scientific importance of studying this era has motivated very large investments (or planned investments) in new NIR facilities (e.g. aboard JWST) that are expected to detect sources at redshifts up to $z \sim 13$ (H -band dropouts), but even they will struggle to find, much less confirm, galaxies beyond this.

To study the origin of the first stars and luminous structures in the universe, observational advances to redshifts exceeding $z \sim 13$ are essential. The exploration of this challenging high- z realm may be enabled by sources that are very bright, and have emission predominantly in the high energy regime, namely GRBs. Their specific advantages are: (i) they likely exist out to the highest redshifts due to their creation in the deaths of massive stars, (ii) the brightest bursts can easily be detected at the highest redshifts due to their huge intrinsic luminosities and energy spectra peaking at ~ 100 – 300 keV; (iii) their pan-chromatic afterglows can also be extraordinarily bright, providing backlights for detailed spectroscopy which is otherwise unprecedented at such distances; (iv) they probe the epoch we seek to understand as their progenitor stars are likely representative of those responsible for the reionisation of the Universe: their current distance record is $z \approx 9.4$ [26]; and (v) a favourable relativistic k -correction implies that they do not get fainter beyond $z \sim 3$. Yet, present and near-future ground- and space-based capabilities are limiting the measurement of redshifts at $z \sim 13$ (as H -band drop-outs), and their afterglows above $2.5 \mu\text{m}$ are too faint by many magnitudes for 8–10 m telescopes.

To fully utilise GRBs as probes of the early Universe one must localise large samples quickly and accurately, and be able to identify which of these are worth the valuable 30–40 m telescope time for detailed study, implying the determination of their (at least photometric) redshifts onboard.

3.1.2 Structure formation scenarios

From studying the cosmic microwave background we know that the Universe started out very simple. It was by and large homogeneous and isotropic, with small fluctuations that can be described by linear perturbation analysis. The present Universe, on the contrary, is highly structured and complicated. Cosmic evolution is thus a progression from simplicity to complexity,

with the formation of the first stars and protogalaxies marking a primary milestone in this transition. Compiling and characterising a sample of very high redshift GRBs will help us directly probe this key phase of cosmic structure formation, as follows.

The first stars that give birth to high- z GRBs must form out of gas that collected inside dense dark matter (DM) potential wells. Structure formation in a cold dark matter (CDM)-dominated Universe is "bottom up," with low-mass halos collapsing first. In the current concordance cosmology, with densities in CDM and dark energy of $(\Omega_M, \Omega_\Lambda) \approx (0.3, 0.7)$ as emerged from WMAP and Planck, DM halos with masses of 10^5 – $10^6 M_\odot$ [27, 28] form from $\sim 3 \sigma$ peaks of the initial primordial density field as early as $z \sim 25$. It is natural to identify these condensations as the sites where the first astrophysical objects, including the first massive stars, were born. Thus, one expects to find GRBs out to this limiting redshift but not beyond. While the standard CDM model has been remarkably successful in explaining the large-scale structures in the Universe and the cosmic microwave background, some discrepancies remain at small scales, $\lesssim 1$ Mpc. Proposed alternatives are either baryonic feedback or Warm DM (WDM; \sim keV particles) models [29]. In the latter case, the resulting effective pressure and free-streaming would decrease structures on small scales [30]. If indeed DM was 'warm', the high-redshift Universe would be rather empty, such that even a single GRB at $z > 10$ would already provide strong constraints on the WDM models [31]. Present constraints rule out WDM particles with masses smaller than 1.6–1.8 keV at 95% confidence level, but depend on assumptions on the slope of the luminosity function and the GRB to SFR rate ratio. Any improvements on these constraints requires a substantially larger number of GRBs with measured redshifts at $z \gtrsim 5$ [32].

On a similar note, GRBs might be used to get independent constraints on the amount of primordial non-Gaussianity in the density field [33]. Deviations from the Gaussian case can only be found at high z .

Measurements of a statistically significant sample of GRBs (minimum ~ 50) at $z > 10$ will therefore help to answer the question:

How were the first structures formed which then developed into the first galaxies?

3.1.3 When and how did the first stars form?

The nature of the first stars in the Universe, and understanding how their radiative, chemical and mechanical feedback drove subsequent galaxy evolution, provide one of the grand challenges of modern cosmology [34]. The earliest generations of stars ended the so-called cosmic dark ages and played a key role in the metal enrichment and reionisation of the Universe, thereby shaping the galaxies we see today

[34, 35, 36, 37]. These so-called Population III (or Pop III) stars build up from truly metal-free primordial gas at extremely high redshift. They have long been thought to live short, solitary lives, with only one extremely massive star with about 100 solar masses or more forming in each DM halo [41, 42, 43, 44]. However, the most recent calculations [45, 46, 47] suggest that Pop III stars formed as members of multiple stellar systems with separations as small as the distance between the Earth and the Sun [48, 49]. Although these recent fragmentation calculations suggest an initial mass function (IMF) that reaches down to sub-solar values, most of the material is probably converted into intermediate mass stars with several tens of solar masses [50, 51]. This agrees with the analysis of abundance patterns of extremely metal-poor stars in the Galactic halo [52], which requires a minimum level of enrichment to form low-mass and long-lived stars [53] and is consistent with enrichment from core collapse supernovae of stars in the intermediate mass range $20 - 40 M_{\odot}$ rather than from pair-instability supernovae of very massive progenitors with $\sim 200 M_{\odot}$ [54, 55, 56, 57, 58].

Second generation stars, sometimes termed Pop II.5 stars, have formed from material that has been enriched from the debris of the first stars. Unlike the very first stars, for which we have no direct detections yet, low-mass members of the second generation may have already been found in surveys looking for extremely metal-poor stars in our Milky Way and neighbouring satellite galaxies. The relative fraction of high-mass stars amongst Pop II.5 stars is still unknown. It is a key question in early galaxy formation to understand the transition from truly primordial star formation to the mode of stellar birth we observe today [59, 60]. When and where did this transition occur? Was it smooth and gradual or rather sudden and rapid? It is therefore important to learn more about the IMF of the first and second generation of stars and to find observational constraints on the star formation process at different redshifts. This would culminate in the more general question:

When did the first stars form, what are their properties, and how do Pop III stars differ from later star formation in the presence of metals?

3.1.4 Detecting high- z objects

Direct detections of Pop III or Pop II.5 stars in the early Universe appear highly unlikely even with upcoming observatories such as the James Webb Space Telescope (JWST) or the proposed 30–40 m ground-based telescopes (such as the E-ELT). Individual stars are much too faint, and only rich clusters of very massive stars might be bright enough to lie above the detection limits in long exposures (e.g. [61]). High-redshift observations seem only able to provide indirect constraints on the physical properties (mass, lu-

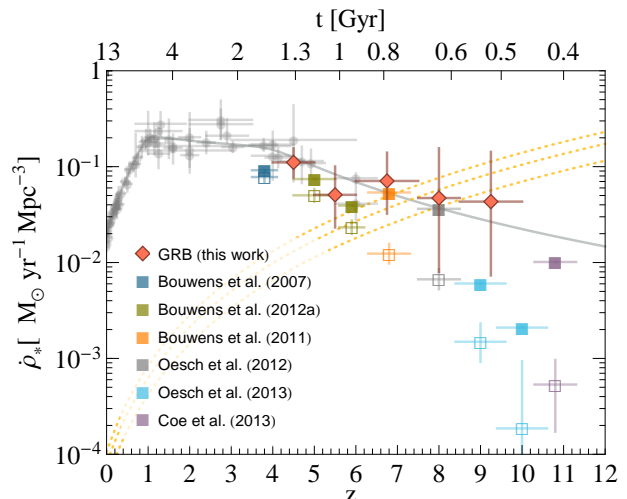


Figure 4: Star formation rate density (SFRD) Low- z data (*circles*) are from [38]. The *diamonds* are obtained using *Swift* GRBs. The *open squares* show the result of integrating the LBG UV luminosity functions down to the lowest measured value, M_{vis} , while the *solid squares* use $M_{\text{cut}} = -10$. All assume a Salpeter IMF. For comparison, the critical $\dot{\rho}_*$ for $\mathcal{C}/f_{\text{esc}} = 40, 30, 20$ ([39], *dotted lines*, top to bottom) are shown. (From [40])

minosity, frequency, etc.) of the first and second generations of stars, for instance, by looking at their influence on reionisation or on the cosmic metal enrichment history [37].

The polarisation data of WMAP, the Wilkinson Microwave Anisotropy Probe (and likely soon the Planck mission) indicate a high electron scattering optical depth, hinting that the first stars formed at high redshift [2, 62, 63]. Massive, low-metallicity Pop III stars may produce very powerful long GRBs [64, 65, 66]. Thus, GRBs offer a powerful alternative route (Fig. 4) to identifying high- z objects, as demonstrated by GRBs 080913 at $z = 6.7$ [67], 090423 at $z = 8.2$ [68, 69] and 090429B at $z = 9.4$ [26]. Indeed, studying GRBs is the only realistic pathway towards the direct detection of Pop III and high-mass Pop II.5 stars and thus towards constraining their mass spectrum as well as their multiplicity. From the predicted mass range of Pop III stars and their high binary frequency it was concluded that a $<0.6\% - 2\%$ fraction of Pop III stars ended their lives in GRBs. While at the *Swift* sensitivity level only $\sim 10\%$ of GRBs detected at $z > 6$ could be powered by Pop III stars, this fraction increases to 40% at $z > 10$ [63]. In addition, both main production channels of GRBs, core collapse supernovae of massive stars (long GRBs) as well as binary mergers involving Roche-lobe overflow and common-envelope evolution (short GRBs) [70], are likely to be present. This makes high- z GRB observations *the* ideal probe of studying early star formation (Fig. 5). The rate of GRBs is expected to track the global cosmic star-formation rate [71, 72, 73] (Figs. 4, 5), though possibly with different efficiencies at high- z

and low- z [74, 75]. Deduced from a principal component analysis on *Swift* GRB data, the level of star formation activity at $z=9.4$ could have been already as high as the present-day one [76], a factor 3–5 times higher than deduced from high- z galaxy searches through drop-out techniques. If true, this might alleviate the longstanding problem of a photon-starving reionisation; it might also indicate that galaxies accounting for most of the star formation activity at high redshift go undetected by even the deepest searches. Clearly, observing more GRBs would be crucial to shrink the currently large error bars at the highest redshifts, thus answering the question:

What is the relation between GRB rate and star formation rate, and what is its evolution with time?

Already with current technology we can characterise GRBs up to redshifts of $z \sim 10$ [26, 68, 69], but reaching larger redshifts requires a new approach and a dedicated mission. The present *Swift* samples of GRBs, both large biased samples as well as smaller but nearly complete samples, indicate a fraction of $5.5 \pm 2.8\%$ GRBs at $z > 5$ [77, 78]. Using standard cosmology and star formation history description (Fig. 4), this translates into a fraction of 1% of all GRBs located at $z > 10$, or 0.1% of all GRBs at $z > 20$ [73]. With 1000 GRBs per year, and a nominal lifetime of 5 yr (goal 10 yr) we would expect 50 (goal 100) GRBs at $z > 10$, and 5 GRBs (goal 10) at $z > 20$. Thus, the measured GRB redshift count will be large enough to observationally constrain the cosmic star formation rate at very high redshifts and it will allow us to determine the earliest cosmic time when star formation became possible - thus answering the question:

What is the true redshift distribution and corresponding luminosity function of long-duration GRBs?

3.1.5 Chemical evolution in the Early Universe

Beside their direct detection, clues about the first stars can be obtained by studying the gas polluted by first supernova explosions [79]. Recent models for the formation of Pop III stars suggest that their typical masses are similar to those of present-day O stars, implying that they will die as standard core-collapse supernovae (CCSNe). However, it is also possible that some Pop III stars may have much larger masses, of the order of a few hundred solar masses. These stars would die as pair-instability supernovae (PISNe), leaving no remnants and producing large quantities of metals and dust [80]. The metal abundance ratios produced by CCSNe and PISNe are quite distinct, and hence by measuring their relative contributions to the metal enrichment of high-redshift gas, we can constrain the form of the Pop III IMF.

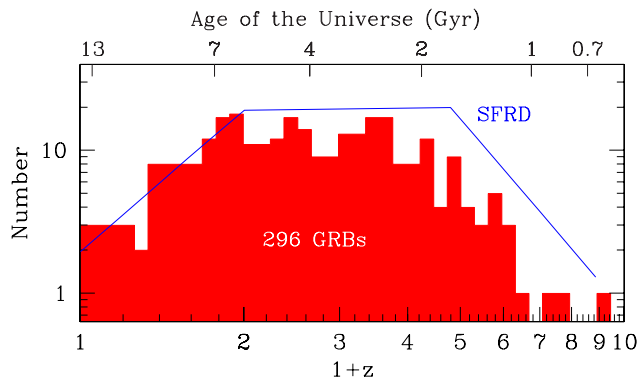


Figure 5: Histogram of the observed number of GRBs (spectroscopic redshift only) per redshift bin by May 2013 (in units of $\log(1+z)$). The number of GRBs increases from $z = 0$ to ~ 1 , is steady up to $z \sim 2.8$, then it decreases down to zero at $z \sim 9$. At low or high z , redshifts are mainly measured from the host galaxy or the DLA detected in the optical afterglow, respectively. Dust (mainly at $z = 1 - 3.5$) and *gamma-ray* flux detection limits (for $z > 3.5$) affect our high- z detections. This is consistent with the comparison with the SFRD (co-moving volume change included) derived from field galaxies [38], scaled to match the observed $z < 1$ GRB histogram. This suggests that a substantial fraction of GRBs at high redshift is presently missed.

GRBs offer a particularly rewarding opportunity to study the physical conditions of the surrounding medium, in various ways. i) The UV radiation of the GRB and its early afterglow ionise the neutral gas and destroy most molecules and dust grains up to tens of parsecs away. Interestingly, rotational levels of molecules and metastable states of existing species (O I, Si II, Fe II) are populated by UV pumping followed by radiative cascades. As the GRB afterglow fades rapidly, recombination prevails and the populations of these levels changes on timescales of minutes to hours, imprinting variable absorption lines in the otherwise flat (synchrotron) afterglow spectrum. This allows us to measure with unprecedented accuracy the density, composition and ionisation state of the surrounding ISM [81]. ii) Other tracers of ionization are molecules forming by the impact of photons (or cosmic rays) on neutral hydrogen, via the formation of H_2^+ , which rapidly leads to the production of H_3^+ and heavier molecules [82]. GRBs, provide a good environment to induce molecule building processes via ionisation. iii) The detection of metals through optical absorption lines in the highest redshift GRBs (e.g., $z=6.3$, Fig. 10) will allow us to determine whether CCSNe or PISNe are primarily responsible for enriching the gas in these high redshift systems. This has important implications for models of the initial stages of reionization [83, 84, 85, 86] and the metal enrichment of the IGM [87, 88], thus answering the question:

When and how fast was the Universe enriched with metals?

3.1.6 The first galaxies

Identifying objects beyond $z \sim 7$ has proven extremely difficult. None of the previously claimed UDF galaxy candidates at $8.5 < z < 10$ could be confirmed by the deeper multi- λ UDF12 campaign [91] (although new candidates were identified). Even if found, such galaxies only represent the tip of the iceberg, in star-formation terms: increasing evidence suggests the bulk of early star formation happened in small, low-mass, and very faint galaxies, inaccessible to optical/NIR surveys. This is illustrated by the finding that, at $z > 5$, six GRB host fields have been observed with deep HST/VLT imaging [19, 92] with null detections in all cases. If no dust correction is applied (dust is not expected to be abundant in the Universe at an age of less than 1 Gyr, especially in small, low metallicity galaxies), the UV luminosity limit can be translated into $\text{SFR} < 2.5 M_{\odot} \text{ yr}^{-1}$ [93]. Particularly remarkable is the deep $m_{AB} > 30.3$ mag NIR limit with *HST* of the host galaxy of GRB 090423 at $z = 8.23$ [19], which gives an incredibly low $\text{SFR} < 0.06 M_{\odot} \text{ yr}^{-1}$.

This finding is in agreement with recent semi-analytic numerical simulations (Fig. 6) that predict that about 70% of GRB hosts at $z > 6$ will be small, with stellar mass in the range $M_{\star} = 10^6 - 10^8 M_{\odot}$, while star formation and metallicity are in the intervals $\text{SFR} = 0.03 - 0.3 M_{\odot} \text{ yr}^{-1}$ and $\log Z/Z_{\odot} = 0.01 - 0.1$, respectively [89]. For comparison, the deepest rest-frame luminosities achieved by the HUDF can only reveal down to $\text{SFR} \sim 0.2 M_{\odot} \text{ yr}^{-1}$ at $z \sim 8$ [94].

Thus, GRBs provide a unique, and above $z \geq 13$ perhaps the only, way of pin-pointing the vast bulk of star-forming galaxies as well as their individual building blocks. Furthermore, the faintness of even the brightest galaxies at $z > 8$ makes spectroscopic confirmation very demanding. GRBs provide the opportunity of probing individual stars at these times, and their afterglows may provide not only redshifts, but detailed information about abundances, gas columns etc. via absorption line spectroscopy. Indeed, *JWST* would be able to obtain $R \sim 3000$ spectroscopy at $S/N \sim 10$ even 7 days after the GRB explosion, while the 30–40 m ground-based telescopes will be able to provide unique information on the chemical enrichment and reionisation history if they can be fed with accurate locations of high- z GRB afterglows (see Fig. 3 for a simulated E-ELT/HARMONI spectrum).

GRB lines-of-sight typically contain more gas than most QSO Damped Ly- α systems (DLAs) as they generally probe dense SF regions within their host galaxies, and in that sense are more representative of high- z star forming environments. It required observation of more than 12,000 DLA absorbers towards $\sim 10^5$ quasars to identify 5 systems with $\log N_{\text{HI}}[\text{cm}^{-2}] \geq 22$ (0.04%, [95]). In contrast, of the 31 DLAs with $\log N_{\text{HI}}[\text{cm}^{-2}] \geq 21.4$ de-

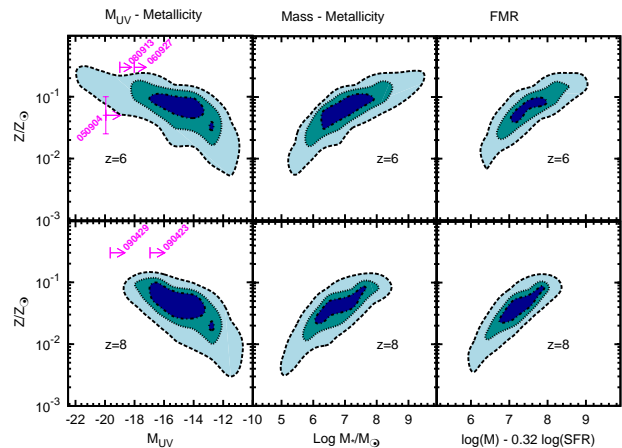


Figure 6: Luminosity-metallicity (left column), mass-metallicity (central column) and Fundamental Metallicity Relation (right column) for the LGRB host galaxy simulations at $z = 6$ and $z = 8$ [89]. Contour plots report the 30%, 60%, and 90% probability of hosting a GRB. Arrows refer to [19] and, in the absence of a measured metallicity, have been positioned arbitrarily at $Z = 0.3Z_{\odot}$, while the metallicity of GRB 050904 has been obtained by [90].

tected in the GRB afterglow population, 35% have $\log N_{\text{HI}}[\text{cm}^{-2}] \geq 22$ (e.g. [96, 97]).

GRBs are already allowing us to see into the heart of star-forming galaxies from $z \approx 0$ to $z > 8$ [68, 69, 98]. With afterglow spectroscopy (throughout the electromagnetic spectrum from X-rays to the sub-mm) we can characterise the properties of star-forming galaxies over cosmic history in terms of mass function, metallicity, molecular and dust content, ISM temperature, etc. Deep follow-up searches for their hosts can then place strong constraints on the galaxy luminosity function, either through weak detections (unlike LBG searches this does not require multi-band photometry for SED fitting), or non-detections which indicate the amount of star formation in undetectable galaxies.

3.1.7 Initial stages of re-ionisation

The reionization of the IGM is the subject of intensive investigation currently, and this is likely to continue for the foreseeable future. The fundamental unanswered question in the field is whether radiation from early stars was sufficient to have brought about this phase change? If not, then we will be compelled to find alternative sources of ionising radiation which, given that emission by quasars seems to fall well short of providing the necessary ionising flux at $z > 3$, may entail new physics such as decaying particle fields. Conversely, if early stars are the explanation, then reionization will teach us about their nature and the time-line of their creation. At the present time it is hard to reconcile the measured star formation with the required ionising background without invoking, e.g., a high Lyman continuum escape fraction, and/or a dom-

inant contribution from a large population of dwarf galaxies (as is, in fact, indicated by studies of high- z GRB hosts [19]), but different from [40].

Various observational windows on the process itself have begun to produce important results. Estimates of the optical depth to electron scattering of the cosmic microwave background (CMB) by WMAP and Planck indicate a reionization redshift of $z \sim 10.4 \pm 1.2$ for an instantaneous reionisation. From an analysis of 17 $z > 5$ quasar spectra it was concluded [99], that the HI fraction x_{HI} evolves smoothly from $10^{-4.4}$ at $z = 5.3$ to $10^{-4.2}$ at $z = 5.6$, with a robust upper limit $x_{\text{HI}} < 0.36$ at $z = 6.3$. However, most limits are model dependent; in fact it was shown that reionization extending to $z < 6$ is not ruled out by current data [84, 100, 101, 102].

In the near future, redshifted 21 cm mapping with LOFAR, MWA and PAPER are likely to better establish the timescale of reionisation, and ultimately much more precisely with SKA. However, the fine-scale topology of the process, and the key question of the nature of the sources responsible for the ionising radiation will remain uncertain. GRBs can provide a unique census of early massive star formation, and a route to understanding the populations of galaxies in which they formed. Crucially, in addition, high-S/N infrared spectroscopy of GRB afterglows can provide simultaneous estimates of the neutral hydrogen column density both in the host [97] and in the IGM surrounding it [103, 104] via the shape of the red damping wing of the Ly α line. While most of the flux on the blue side of Ly α is simply absorbed for a wide range of neutral fractions, the shape of the red wing depends on the neutral hydrogen fraction of the IGM in which the source is embedded, the host neutral column and the extent of any Strömgren region around the host [105]. Although this is complicated by the requirement to disentangle the HI absorption in the host from that in the IGM, in principle, it can be done as exemplified by GRB 050904 at $z = 6.3$ despite a low-S/N spectrum and high host N_{HI} (Fig. 10) [106]. A large sample of high- z GRBs will likely provide a fraction of absorbers with low column density, allowing us to cleanly isolate the IGM damping wing. The scatter in the IGM absorption from an inhomogeneous reionisation is itself a robust reionisation signature, which can be statistically isolated in a reasonably large GRB sample [107]. The exciting prospects for such studies in the era of 30–40 m ground-based telescopes is illustrated by the simulation in Fig. 3.

Thus, a sample of a few dozen GRBs at $z > 8$ would constrain not only the progress of reionisation, but its variance along different lines of sight (which may be correlated with identified galaxy populations at the same redshift), and also the typical escape fractions of radiation from early massive stars. The latter is a crucial, but extremely hard to quantify, piece of the puzzle, since only if the ionising radiation can escape

unimpeded from a significant fraction of massive stars (say, $> 20\%$), will they be successful in driving reionization. Measuring directly the neutral columns to many GRBs will establish how many lines of sight provide such an unabsorbed view. With a fiducial GRB-finder with 1000 GRBs/yr and immediate redshift estimates, ground-based spectroscopy can be secured for many dozen GRBs in the $6 < z < 13$ range. An unique and independent way of probing the high- z UV radiation field with GRBs is through its effect on high-energy photons. The expected UV field at these redshifts can cause appreciable attenuation above a few GeV, that can be observable with e.g. CTA [108]. In conclusion, a powerful GRB detection and localisation mission, in tandem with future facilities expected to be available on a 15–20 year time frame, will answer the question:

How did reionisation proceed as a function of environment, and was radiation from massive stars its primary driver?

3.1.8 Warm-hot IGM studies

The redshift distribution of X-ray absorbing column densities, N_{HI} , as detected in GRB afterglows by *Swift*/XRT shows a significant excess of high N_{HI} values at redshifts $z \geq 2$ with respect to the low redshift GRBs [109, 110, 111]. This excess absorption has been tentatively interpreted as due to the presence of absorbing matter along the line of sight not related to the GRB host galaxy. This can be either diffuse (i.e. located in diffuse structures like the filaments of the Warm-Hot Intergalactic Medium - WHIM [112, 113]) or concentrated into intervening systems (i.e. galaxies or clouds along the line of sight [109, 110]). The study of X-ray absorptions for a larger sample of GRBs at redshifts $z \geq 2$ could provide new insight on the nature of the intergalactic medium and in particular allowing to constrain its metal content.

Quasars are the alternative target for this kind of studies, in fact WHIM signatures have been detected when observing the bright blazar Mkn 421 (e.g. [114]). GRBs provide a much larger flux, if observed promptly, allowing us to extend these studies to larger distances. It is not easy to disentangle filaments from intervening systems, whereas a sufficient spectral resolution will allow us to detect distinct absorption features (originating at a given redshift) versus a truly diffuse medium (across a redshift range). As a by-product a direct measurement of the GRB redshift can be obtained from the X-ray data alone [115].

3.2 The GRB origin

3.2.1 GRBs and neutrinos

Neutrinos are electrically neutral, weakly interacting elementary particles which are produced as the result of radioactive decay, nuclear reactions or proton-proton collisions. Examples are the fusion reaction in

the Sun, electron capture during the collapse of stars into a supernova, and particle acceleration (jets) in e.g., active galactic nuclei, microquasars, supernova remnants or GRBs [116]. Due to the very small interaction cross section, neutrinos are difficult to detect, but the detection sensitivity increases dramatically with neutrino energy. This disadvantage is however an advantage for the search for neutrinos at the same time: they are neither absorbed nor deflected on their way to Earth, so that the production region can be studied. This makes them unique in the search for the origin of ultra-high energy cosmic rays.

The vast majority of the neutrinos from a GRB is emitted at moderate energies (~ 20 MeV) from the central engine's accretion disk. Their moderate energies together with the steep energy dependence of the interaction cross sections make them hard to detect. Chances are much better for those neutrinos produced by the ultra-relativistic outflow that is responsible for the GRB prompt emission. The GRB fireball phenomenology predicts spatially and temporally correlated neutrino emission to occur from proton-proton or proton-photon interaction. For a neutrino flux distributed as a power law $\propto E^{-2}$, this implies that energies in the range TeV to PeV are most promising for neutrino detection from distant sources [117].

A number of possible neutrino production sites from long GRBs have been identified: within the exploding star, within the relativistic outflow, and within the reverse shock that is formed as the afterglow is developing. Neutrinos can be formed in proton-proton and proton-photon interactions in the jet cavity that is formed as the jet penetrates the collapsing star. This is expected to produce a flash of neutrinos with energies of 3 – 10 TeV. Alternatively, neutrinos can be produced in the same region as the γ -ray photons, within the jet. Here, the so-called prompt neutrino emission with energies of ~ 100 TeV should accompany the γ -rays. The detailed timing of neutrino and γ -ray emission can constrain the physics of the GRB emission.

Despite sophisticated searches, neutrinos from GRBs have not been detected so far. While our best hope for neutrino detection is with the continued operation of IceCube until (at least) 2020, the follow-up project KM3NeT is in its extended design phase, with the implementation of the first phase of the infrastructure being immanent. The neutrino detection from GRBs would clarify the hadronic content in GRB jets. Moreover, systematic measurements of the neutrino energies, in particular if they peak at certain key energies, could help discriminate between models, even more so when combined with properties of the measured γ -ray spectrum. A neutrino detection from GRBs would also directly prove GRBs as sources of ultra-high energy cosmic rays. The ratio of neutrinos to γ -rays, typically produced in similar numbers, would provide indications, otherwise difficult to obtain, on the attenuation of γ -rays in the early stages of the fireball.

Detection of neutrinos from cosmologically remote GRBs (i) provides limits on the lifetime of the dominant mass eigenstate by a factor >200 better than for SN 1987A; (ii) is a testbed of neutrino properties with an unprecedented accuracy; (iii) tests if neutrinos follow the weak equivalence principle; (iv) facilitates the exploration of quantum-gravity-induced Lorentz invariance violation; (v) provides tremendous advantage over other methods of studying cosmology, as neutrino flavor ratios should be independent of any evolutionary effects.

In addition to those microphysics-related goals, the detection of high-energy neutrinos from GRBs aims at answering the astrophysical questions of the (i) identification of the sources of ultra-high energy cosmic rays; (ii) determination of the ratio of accelerated electrons to protons in GRBs, (iii) proper treatment of the GRB jet physics, including hadronic cosmic rays. In order to achieve those central goals, neutrino telescopes rely heavily on satellites that trigger GRBs: neutrino analyses can improve their sensitivity by reducing the main background of atmospheric neutrinos to almost zero through the selection of events in space and time, according to the occurrence of GRBs. This makes the GRB analysis one of the most sensitive ones for cosmic neutrinos. Only with existing satellite triggers, we can answer the question:

How are γ -ray and neutrino flux in GRBs related, and how do neutrinos from long GRBs constrain the progenitor and core-collapse models?

3.2.2 GRBs and gravitational waves

Short GRBs (sGRBs) and GWs are linked by the common topic “compact binary mergers” and they nicely illustrate how complementary and mutually beneficial the information obtained in both channels is [118, 119]. Moreover, the additional EM signals expected from a compact binary merger provide a close link to cosmic nucleosynthesis.

About one quarter of the *CGRO/BATSE* and *Fermi/GBM* bursts are classified as short-duration (< 2 s), hard GRBs. As short GRBs are intrinsically less luminous in EM radiation than their long-duration cousins, the observed sample is dominated by relatively nearby sources. The presently known redshift distribution suggests that a detection rate of 1000 GRBs/yr corresponds to 10–15 short GRBs/yr at $z < 0.1$ (~ 450 Mpc) [11, 120], depending on the energy range of the trigger instrument.

The question of their central engine is a long-standing puzzle. Compact binary mergers (either NS-NS or NS-BH) are the prime suspects, but this connection is far from proven. The coincident detection of a sGRB and a GW signal could finally settle this issue. The network of the gravitational detectors Advanced *LIGO/VIRGO*, soon complemented by LIGO-India and KAGRA is expected to deliver the first direct GW detections within a few years from now. It

will be capable of identifying an optimally oriented NS-NS (NS-BH) merger out to ~ 450 (~ 900) Mpc, with a combined predicted rate of the order of 50 yr^{-1} [14]. The GW signal of a compact binary merger potentially delivers a wealth of information on the physical parameters of the binary system. For example, it provides the neutron star masses and radii, it carries the imprint of the equation of state at supra-nuclear densities, and it constrains the collapse stages, e.g., through a hypermassive NS or magnetar to a BH, information that is hardly accessible otherwise. Comparison of the rates of GW detections with and without sGRB counterparts may constrain the geometry of the relativistic outflow (“jet”), the source energetics and the physical emission processes. But while providing a clear view on the physics of the actually merging system the poor localizations by GWs of ≈ 10 –1000 square degrees [12, 121] leave us nearly blind with respect to the astrophysical environment in which the merger takes place.

A complementary EM detection can provide a wealth of additional information. Firstly, it locates the source for optical follow-up providing an accurate localization relative to the host galaxy, thus allowing us to study the environment of such evolved sources. This, in turn, constrains binary stellar evolution by providing information on kick velocities, initial separations etc. Secondly, a redshift and thus luminosity determination combined with the absolute source luminosity distance provided by the GW signal can deliver precise measurements of the Hubble parameter (10 GW+EM events in Advanced LIGO/Virgo may constrain the Hubble parameter to 2-3% [122], and ET will constrain it to $<1\%$ [123]), and hence help to break the degeneracies in determining other cosmological parameters via CMB, SNIa or BAO surveys. Thirdly, the detection of a radioactively powered transient [124] may provide an interesting link to cosmic nucleosynthesis: this could show the “r-process in action” and finally settle the question of where the heaviest elements around the platinum peak (nucleon numbers $A \sim 195$) come from. Neutrino-driven winds from a merger remnant [125] may lead to yet another radioactive transient, but with likely different properties. Once the matter that is dynamically ejected interacts with the ambient medium it may produce radio flares which independently would set a limit on the merger rate [126].

The localisation of GW events has another more subtle benefit: it improves the accuracy with which parameters can be estimated from the GW observation [127]. The covariance of angular errors with uncertainties in other parameters (distance, polarisation, stellar masses etc) is usually significant. Thus, a more accurate position through EM follow-up also improves the determination of all the parameters measured gravitationally. For short GRBs, several of the GW events will be near threshold, and because the

GW amplitude is peaked along the jet axis, the detection range increases by a factor of ~ 2 with coincident detection of a short GRB X-ray afterglow [128].

Only with a sensitive GRB detector in orbit, operating in conjunction with the gravitational wave detectors, can we answer the question:

Can short GRBs be unambiguously linked to gravitational wave signals, and what do they tell us about the neutron star merger scenario?

3.2.3 Gamma-ray polarisation

Until 5 years ago, the prompt 20–1000 keV emission was interpreted as a smoothly broken power law produced by synchrotron emission. Recent discoveries of additional spectral components at high and low energies with *Fermi*, as well as γ -ray polarisation measurements with *INTEGRAL* and *IKAROS* have dramatically challenged our view of the GRB emission process. Is the broken power law a Comptonised thermal component from the photosphere? Is the high-energy part produced by inverse Compton radiation and the low-energy component of synchrotron origin? Time-resolved γ -ray polarimetry of the GRB prompt emission would be a unique discriminant of the underlying physics. The level of polarisation will depend on the radiation mechanism as well as geometrical effects. In particular, it will probe the strength and scale of the magnetic field. A significant level of polarisation can be produced by either synchrotron emission or by inverse Compton scattering. The fractional polarisation from synchrotron emission in a perfectly aligned magnetic field can be as high as 70–75% [129, 130]. An ordered magnetic field of this type would not be produced in shocks but could be advected from the central engine [129, 131]. Strong correlations are predicted between the polarisation level, the jet Lorentz factor and the power-law index of the particle distribution [132]. Another asymmetry capable of producing polarisation, comparable to an ordered magnetic field, involves a jet with a small opening angle that is viewed slightly off-axis [133]. In the case of photospheric emission, as recently hotly debated based on *Fermi* data, polarisation can arise due to the multiple Compton scatterings before photons escape [134]. Measurements of the temporal evolution of both, the degree of polarisation as well as the polarisation angle have strong diagnostic power to constrain GRB models.

Recently some measurements of polarisation during the prompt emission of GRBs in the hundreds of keV energy range have been reported [135, 136, 137, 138, 139, 140, 141]. Although all these measures, taken individually, have not a very high significance ($\gtrsim 3 \sigma$), they indicate that GRBs may indeed be emitters of polarised radiation. In particular, the changing polarisation angle with time [138, 140] indicate a fragmented jet. This kind of polarisation measurements can shed

new light on the strength and scale of magnetic fields, as well as on the radiative mechanisms at work during the GRB prompt emission phase.

In addition, polarisation measures in cosmological sources are also a powerful tool to constrain Lorentz Invariance Violation (LIV), arising from the phenomenon of vacuum birefringence as shown recently [141, 142, 143, 144].

The next generation of instruments will be sensitive enough to not only provide averaged polarisation angles and degrees for each detected event (long and short bursts), but even more pulse-resolved measurements for the brighter events. The detailed analysis of the prompt emission polarisation properties in GRBs would lead to essential clues to the emission mechanism. In particular, an ordered magnetic field can be determined or ruled out.

3.3 Time-domain astrophysics

It is now widely accepted that the next astronomical discovery frontier is the time domain (as emphasised in the Astronet Roadmap and in the US Decadal Survey). Current time-domain experiments are extremely successful and the coming years will see a revolution in time-domain astronomy with many surveys in the optical and in the radio.

3.3.1 Other high-energy transient types

Besides GRBs, also other transient source classes can trigger instruments surveying for GRBs. Transient high-energy sources, watched in real-time, offer insight into the physics of accretion, the presence (and mass) of BH in galaxies, and the behaviour of matter under extreme gravitational and magnetic fields, to name but a few. While much science in these diverse subjects arises from detailed follow-up across the EM spectrum, many of the events are most dramatic at higher energies, and hence require high-energy triggers to identify, even in the era of LSST.

Within the Milky Way our proposed mission will be sensitive to emission from M-dwarf stars, mapping out the frequency of their activity and the implications for planet habitability (especially important as many next generation planet searches are targeting M-dwarfs due to improved contrast). We will pinpoint soft gamma-repeaters – highly magnetised neutron stars that are possible gravitational waves sources and which provide a test bed for physics in both strong gravitational and magnetic fields, and for models of the supernovae that may create them. Outbursts from X-ray binaries of various types are also likely to be discovered, potentially even from outside the Milky Way.

The breakout of the SN shock from the star might provide a short lived, but luminous X-ray burst, that has likely been observed in at least one case (SN 2008D). More generally, SN can create powerful X-rays via

their interaction with the circumstellar medium, offering a route to studying mass loss in the years before the stars demise. X-rays might also be generated from engine-like events deep within the ejecta that become visible at late times as the ejecta becomes optically thin. Of particular importance is the nature of the superluminous SN [145], whose origin may be similar to the dominant mechanism thought to operate in Pop III stars, and which have recently been claimed to be (at least occasionally) powerful X-ray emitters.

Moving further out into the Universe we can study more massive black holes in galactic nuclei. The recent discovery of hard high-energy emission from Swift J1644+57 [146] suggests that tidal disruption flares (TDFs) might be powerful high-energy transients, while it is also thought that all TDF produce softer thermal X-ray emission [147]. TDFs offer a unique route to probing BHs in galaxies, including their location and ubiquity within dwarf galaxies (where it is far from obvious they reside), hence they allow us to extend the relation between BH mass and stellar velocity-dispersion to much lower masses, providing strong constraints on galaxy evolution models. Finally, these events allow us to study accretion around supermassive BHs from switch on to switch-off in human timescales, much shorter than the millions of years in which active galaxies evolve.

3.3.2 Complementarity with other transient detection systems

The main reason for the community-wide focus on the transient and dynamic Universe is that it is most often associated with extreme physical phenomena: eruptions on a stellar surface, complete explosion of a star, "shredding" of a star by a supermassive black hole, merger of two extremely compact objects, etc. These phenomena most often emit non-EM signals, in particular cosmic rays, neutrinos and gravitational waves. Our proposed mission concept would detect and localise energetic phenomena that are most likely to be associated with non-EM signals.

By definition, the transient sky is unpredictable which is why all EM facilities have a very large field of view; the need for very wide area coverage cannot be overstated, and it is crucial to have an EM monitor that sees a large fraction of the sky all the time. We can do this with a dedicated γ -ray mission. Focussing on one wavelength range or one information carrier (e.g., EM, GW, ν) is like having a black-and-white picture: there is useful information but we are missing something. A range of instruments covering the whole EM spectrum in conjunction with other information carriers will give us a detailed *color* image, allowing us to see the whole physical picture, thus addressing the question:

What are the electromagnetic counterparts to gravitational waves and neutrino bursts?

4 Requirements for enabling instruments

Both, the use of GRBs as a tool as well as the simultaneous detection of an EM signal with a GW/neutrino signal, requires an in-orbit trigger and search facility (“GRB-finder”) that can simultaneously localise the event within the large error boxes provided by the GW (and neutrino) facilities.

In order to use GRBs as a tool, positions with arcsec accuracy are required. The localization accuracy of the GRB-Finder will not be sufficient, and thus an X-ray and/or optical/(N)IR telescope is required which is rapidly slewed to the position determined by the GRB-Finder. An X-ray telescope is preferred since the sky is too crowded at optical/(N)IR wavelengths. Finally, to tackle the early Universe questions and obtain decent statistics at $z > 10$, a next-generation GRB mission should detect of order 1000 GRBs/yr, providing 50 (5) GRBs at $z > 10$ (20) over a 5 yr mission lifetime. This high GRB rate requires a pre-selection of ‘interesting’ events, and therefore a (N)IR telescope is foreseen which will determine redshifts for the bulk of the high-redshift (e.g., $z > 7$) sources. Table 1 summarises these high-level requirements.

4.1 The GRB-finder

The localisation accuracy and timeliness are the crucial parameters when aiming at follow-up observations at longer wavelengths. We discuss in the following only concepts which provide localisations better than a few degrees within minutes after the GRB. In general, as the prompt GRB spectral slope is -1 in the 1–100 keV band, lowering the energy threshold allows for the detection of a larger number of GRBs.

Scintillation detectors: The use of simple scintillator detectors like *CGRO/BATSE* or *Fermi/GBM* has, in the past, only led to afterglow identifications for a handful of GRBs, due to their large localisation uncertainties. The systematic error for *GBM* bursts is 3.3° for $\sim 90\%$ of the cases, with a tail of 12.5° for the rest. The twelve NaI detectors on *Fermi/GBM* work in the 8–1000 keV band, and with an effective area of about 100 cm^2 each in the 20–50 keV band they detect ~ 270 GRBs per year [148]. Increasing the rate to our fiducial 1000 GRBs/yr can be achieved in different ways. Firstly, if flown in, e.g., a L2 orbit, the lack of the Earth occulting half the sky implies doubling the detection rate. Secondly, increasing the effective area by simply using larger crystals is straightforward. Scaling the background rate appropriately and assuming the same S/N ratio for triggering, an effective area of $10\times$ that of *GBM* would provide 1000 GRBs/yr in a low-Earth orbit (LEO).

Coded Mask Instrument: Such systems have been widely used in space for detection of GRBs (e.g. *Swift/BAT*), and work in the ~ 2 –200 keV band. Their advantages are: i) observe over a large solid angle;

ii) can use hard X-ray/ γ -ray detectors to cover quite large energy bandpass; iii) can give fairly good localisations (one to few arcminutes); iv) provide a large number of photons, allowing easier spectral analysis. Disadvantages are: i) they are non-focussing, so sky background prohibits the detection of faint sources or monitoring of fading emission from sources which trigger the instrument (i.e. this requires an additional focussing telescope which can create a data gap – as in the case of *Swift* – while the satellite slews); ii) while coded mask instruments can be used with large-area Si detectors to cover the X-ray band, they have a modest bandwidth (2–50 keV).

Simulations using the presently known $\log N$ - $\log S$ relation and luminosity function of GRBs [75] reveal the following trade between depth and area of a coded-mask similar to *Swift/BAT*: aiming at 2 (4) times the depth of *BAT* gives a similar number of high-redshift GRBs as increasing the detector area by a factor of 2.5 (5). In order to achieve ~ 1000 GRBs/yr, a system of seven *BAT*-like systems with only modestly increased ($1.4\times$) effective area would be necessary (or correspondingly enlarged versions of the advanced coded mask instruments *SVOM/ECLAIRS* or *UFFO/UBAT*).

Lobster Optic Instrument: The use of a wide-field Lobster Eye (LE) Microchannel Plate (MCP) or Multi-Foil (MFO; [149, 150]) imaging instrument provides several advantages over traditional coded mask wide-field telescopes: i) one gets continuous monitoring in a single bandpass (i.e., no gaps due to slews) as the same telescope finds and then continues to monitor the transient; ii) the use of a focussing optic lowers the sky background against which sources are detected, increasing the sensitivity by about two orders of magnitude; iii) ability for good localisation ($< 1'$ down to about $10''$) particularly for higher focal lengths; iv) multiple, lightweight modules can be utilised to cover large solid angles. The principle disadvantage is the need of (modular) large area detectors (as for coded mask telescopes). LE instruments are restricted to low energies (of order 0.5–10 keV). At similar mask/optics area and FOV, a Lobster optics would detect about 3 – $4\times$ more GRBs than a coded mask system [151]. A detection rate of 1000 GRBs/yr could be reached with about 10 modules of the type proposed for the Lobster mission [152].

Compton Telescope: A Compton telescope would work at higher energies (~ 200 keV to ~ 50 MeV), and has the advantages of i) uniquely excellent gamma-ray polarisation capability, and ii) a wide energy band. The disadvantage is a localisation accuracy substantially poorer than a coded mask or Lobster optics instrument, of order 1° radius only, and a rather large mass. An existing concept of such a detector promises ~ 600 GRBs/yr [153], close to our 1000 GRBs/yr goal.

Table 1: Scientific requirements for a future GRB mission with assumed 5 yr lifetime.

Requirement	Goal	Detector ability
1. Detect 1000 GRBs/yr	obtain 50 (5) GRBs at $z > 10(20)$	large FOV, soft response
2. Rapid transmission to ground	allow timely follow-up observations	communication network
3. Rapid localization to few "	opt/NIR identification of 1000 GRBs/yr	slewing X-ray or opt/NIR telescope
4. Provide z -indication	allow selection of high- z objects	multi-filter or spectroscopic capability

4.2 The X-ray telescope for precise localisation (and spectroscopy)

The main driver for the design of the X-ray telescope (XRT) is the position uncertainty provided by the GRB-finder, such that the full GRB error circle can be covered. In addition, the sensitivity should allow all GRB afterglows to be detected. Scaling from the *Swift/XRT* detections of the faintest GRBs, and considering the goal of reaching substantially larger redshifts (and thus likely fainter afterglows), the XRT should be a factor ~ 3 more sensitive than *Swift/XRT* (Fig. 7). Such sensitivity requirement (of order 10^{-13} erg/cm²/s in 100 sec) excludes coded mask systems. In case of a Compton telescope as GRB-finder, a FOV of 3° diameter is needed. Combined with the sensitivity requirement, a single-telescope Wolter-I optics is problematic. A practical solution is to adopt the *eROSITA* scheme of 7 Wolter-I telescopes, and adjust their orientation on the sky such that they fill the required FOV. For the other two GRB-finder options a single *eROSITA* telescope would be sufficient, or alternatively the *XMM* flight spare (though larger and more massive). Simpler versions like an enlarged version of the *SVOM/MXT* or a long focal-length Lobster are possible as well, with the trade-off of less versatile auxiliary science options as compared to *Swift/XRT*.

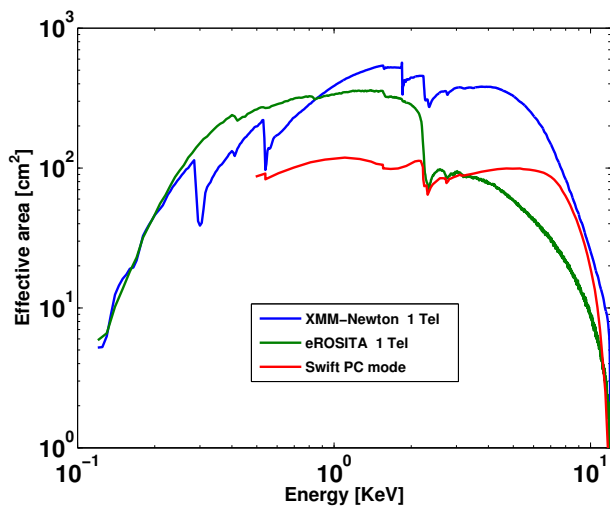


Figure 7: Comparison of the effective area of a modified *eROSITA* system (one telescope per sky position instead of all 7 telescopes co-aligned) with those of *XMM* and *Swift/XRT*. (From [153])

4.3 The (N)IR telescope

The main driver for the design of the Infrared Telescope (IRT) is the goal to (i) detect and accurately localise the counterpart, and (ii) measure the redshift to an accuracy of at least $\Delta z/z \sim 0.2$, so that high- z GRBs can be quickly identified for detailed follow-up study. Above redshift $z \sim 17$, Ly α is moving out of the K -band. This and the requirement to be sensitive up to redshifts of ~ 30 imply to observe in the L ($3.5 \mu\text{m}$) and M ($4.5 \mu\text{m}$) bands.

Based on a complete sample of GRB afterglow measurements obtained with the 7-channel optical/NIR imager GROND since 2007 (update of [77]), in particular the brightness distribution in each of the JHK channels, a minimum afterglow brightness of $M(\text{AB}) \approx 22$ mag at ~ 1 h after the GRB is deduced (Fig. 8). Such sensitivity will be reached with the future 30 m class telescopes, but since it is illusory to follow-up 3 GRBs/night with those instruments, we consider this an onboard requirement in the following.

Using standard parameters for the transmission of the optical components, read-out noise of the detector as well as zodiacal background light, a 1 m class telescope would achieve at least a 5σ M -band detection of each GRB afterglow with a 500 sec exposure when observed within 2 h of the GRB.

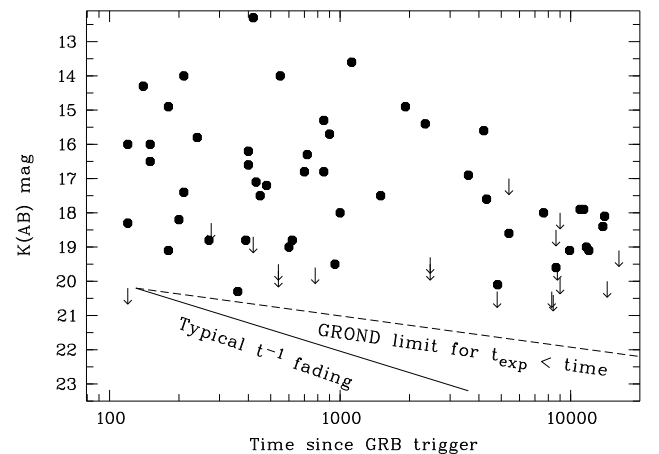


Figure 8: K -band photometry of a complete sample of GRB afterglows based on GROND data. At 1000 s after the GRB, 95% of the afterglows are brighter than $K(\text{AB})=22$ mag. With $K - M \sim 0.8$ mag for typical afterglow spectral slopes, we aim at $M(\text{AB})=21.2$ mag at 1000 sec, or $M(\text{AB})=22.2$ mag at 1 hr after the GRB.

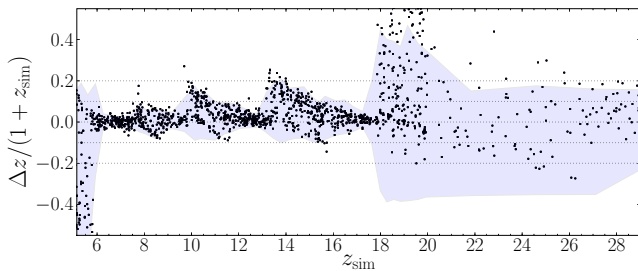


Figure 9: GRB afterglow photometric redshift accuracy of a $zYJHKLM$ filter set. Small black dots show a mock set of 900 simulated afterglow spectra and their corresponding photo- z . The blue-shaded area shows the quadratic sum of the typical difference to the input redshift and the 1σ statistical uncertainty of the photo- z analysis averaged over 30 afterglows in relative ($\eta = \Delta z/(1+z)$) terms. For the $7 < z < 17$ redshift range, the photo- z can be determined to better than 20%. At $z > 17.5$ (K -dropout), the error gets larger due to the gap above the K band and the widths of the L (M) bands; yet, the redshift accuracy is more than sufficient for any follow-up decision.

The inclusion of the LM bands into the IRT requires operating temperatures of about 37 (50) K for the M (L) channels. This will certainly require active cooling. In addition, several optical elements in the optical path will have temperature constraints, so that the thermal architecture of the instrument will need to be designed carefully, though it will be much less stringent than e.g. on Herschel.

After the slew to a GRB, the XRT will provide a position with an accuracy between $5\text{--}20''$ depending on the details of the XRT and the off-axis angle of the GRB in the XRT FOV. This uncertainty is too large for immediate (low-resolution) spectroscopy, so two options are possible.

The simple and cheap option is a simultaneous multi-band imager in, e.g., the seven bands $zYJHKLM$ [153], thus covering the redshift range $7 \lesssim z \lesssim 30$. Since GRB afterglow spectra are simple power laws, and at $z > 3$ Lyman- α is the dominant spectral feature, relatively high accuracies can be reached even with broad-band filters (Fig. 9), as demonstrated in ground-based observations with GROND [154].

A more sophisticated, but also more sumptuous option is a combined imager and spectrograph, as proposed for the dedicated GRB mission ORIGIN [155]. Different areas of the detector are used for either imaging in (sequentially exposed) multi-band filters, low-resolution ($R=20$) spectroscopy, or high-resolution ($R=1000$) integral-field spectroscopy. Switching between these modes requires few arcmin re-pointings of the satellite, based on an accurate position derived from initial imaging data. The power of a $R=1000$ NIR spectrograph on a 1 m space telescope is demonstrated in Fig. 10, allowing unique absorption line diagnostics for $\sim 50\%$ of the GRBs up to the highest redshifts.

5 Strawman mission concepts

5.1 A Distributed Approach

As with other areas of research, the next step forward in understanding GRBs or using them as a tool requires a substantial larger effort on the instrumentation. The basic idea behind this distributed approach is our conviction that strategically linking together future large/expensive global facilities (both ground- and space-based) is of considerable importance to maximise the overall scientific return, in particular at the ever growing costs with more and more ambitious projects. In a perfect world, the different major funding agencies could be expected to seriously weigh up the possible synergy in making their selections.

Separating the tasks: The GRB-finder and the two narrow-field instruments do not have to share the same satellite. In fact, the rapid slewing of the X-ray and (N)IR telescopes is optimised if the flight configuration has low mass (angular momentum). A concept study with EADS Astrium indeed showed that a 2-satellite configuration flight would be preferable even in a LEO (at 500–2000 km distance, not requiring precision formation flying!) unless the GRB-finder is very simple and light-weight. Thus, a strawman concept would be (i) one satellite with a GRB-finder, and (ii) another satellite combining the XMM or $eROSITA$ spare with an $EUCLID$ -sized telescope (just M1 to M3 mirrors, and at largely reduced optical quality and alignment requirements). The GRB-finder with the largest impact on auxiliary science would be a “super-BAT”, i.e. an octahedron-shaped satellite where all but the Sun-facing direction contain a coded mask telescope with 2000 cm^2 detector area each. Being placed in L2, and with no slewing required, such a configuration would detect ~ 1200 GRBs/yr. The follow-up satellite would slew to each GRB and observe for $\approx 1\text{--}2$ h minimum time. This would allow up to 15 GRBs to be observed on a single day (occurring once or twice per year), but on average could leave about half the observing time of the X-ray/(N)IR telescopes to other science areas. Data could be sent to the GRB-finder (or other geostationary satellites) from where it would be much easier to rapidly down-link to Earth due to the fixed location in space.

Piggyback on ESA missions under consideration:

An alternative option could be to add a GRB-finder to one of the ESA missions already under discussion. This would provide Table 1 items (1) and (2), possibly even (3) for a subset of GRBs. Providing (3) and (4) would require either a dedicated mission or a smaller follow-up mission. We acknowledge that these are substantial modifications to the existing concepts.

(1) Adding a GRB-finder to ATHENA+ (or other L2-selected mission) and prepare for reasonably rapid (2 h) autonomous slewing capability: The presently planned ATHENA+ Wide-Field Imager has a FOV

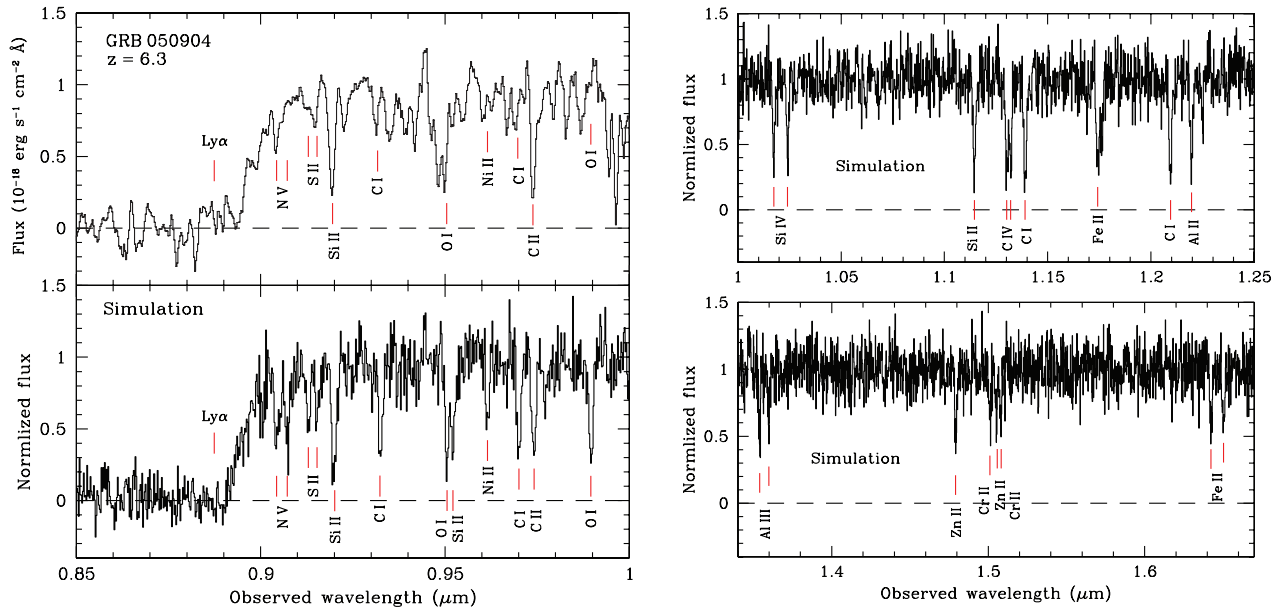


Figure 10: Spectrum of the afterglow of GRB 050904, taken with Subaru/FOCAS 3 days after the GRB (top left; [90]), and simulation of a $R=1000$ spectrum taken with a space-borne 1 m telescope for 1 hr exposure at an afterglow brightness of $J(AB)=21$ mag (lower left panel with the same wavelength range as the observed spectrum, and the J - and H -band regions in the right panels). A metallicity similar to that of GRB 050904 is assumed, with a ZnII column of $2.5 \times 10^{13} \text{ cm}^{-2}$, and ionised gas (e.g. AlIII, CIV, SiIV) with a column of 1/10 of the neutral gas.

large enough to cover several-arcmin sized GRB error boxes, and the calorimeter would provide unique X-ray absorption spectra for the line-of-sights to GRBs. In such a scenario, a separate (N)IR telescope would be needed.

(2) Similarly, adding a GRB-finder to the Large Observatory For X-ray Timing, *LOFT* [156]: *LOFT* is expected to detect of order 150 GRBs/yr, which is too few for the purpose proposed here. Since autonomous slewing is not part of the *LOFT* concept, an enhancement of the GRB-finder capabilities would imply that a separate satellite with the X-ray and (N)IR telescope would be required.

5.2 All-in-One mission

We see the following options (though other mixing and matching of these components would also be possible), determined by the properties of the GRB-finder (field-of-view and localization accuracy). Most of these configurations, if not all, would benefit from an L2 orbit which therefore is taken as the default option. Depending on the combination, up to three autonomous slews will be needed to achieve (N)IR spectroscopy of the GRB afterglow.

Scintillator, single Lobster, NIR: Using a GBM-like detector with $4 \times$ larger effective area, and 20–24 modules will cover the full sky and return 1000 GRBs/yr with locations in the 1° – 4° range. Autonomously re-pointing a long focal length (~ 2 m), narrow-field ($8^\circ \times 8^\circ$) Lobster provides a 95% detection rate of the X-ray afterglows, and a position accu-

rate to <0.5 – $1'$. This position is good enough for the (N)IR telescope to slew and start 7-channel imaging and obtain a $1''$ position. Another slew would place the afterglow on the spectrograph.

All-sky Lobster, XRT, NIR: Using about a dozen short focal length (thus small effective area), large-FOV ($30^\circ \times 30^\circ$) Lobster modules would detect about 1000 GRBs/yr with locations accurate to few arcmin. Autonomously re-point a single *eROSITA*-like X-ray telescope to get a 99% X-ray afterglow detection rate, and localizations accurate to $\lesssim 30''$, accurate enough for (N)IR 7-channel imaging and/or grism spectroscopy. Possibly, a longer focal length Lobster could replace the *eROSITA*-like X-ray telescope.

Coded mask, XRT, NIR: Using eight Swift/BAT-like coded mask systems in octahedron orientation, and lowering the low-energy threshold from 20 to ~ 10 keV would provide 1000 GRBs/yr with locations accurate to few arcmin. Autonomously re-point a single *eROSITA*-like X-ray telescope to get a 99% X-ray afterglow detection rate, and localizations accurate to $30''$, accurate enough for (N)IR 7-channel imaging and/or grism spectroscopy.

Compton, XRT, NIR: Two systems of half a cubic-meter Compton telescopes (e.g. [153]), oriented in opposite directions, will detect about 1300 GRBs/yr, out of which about 900 will have localisations $<1^\circ$. Autonomously re-point of seven *eROSITA*-like X-ray telescopes, oriented to fill a 3° diameter FOV, will provide a 99% X-ray afterglow detection rate. The $30''$ localizations are accurate enough for (N)IR 7-channel imaging and/or grism spectroscopy.

References

- [1] Lamb D.Q., Reichart D.E., 2000, ApJ 536, L1
- [2] Naoz S., Bromberg O., 2007, MN 380, 757
- [3] Hjorth J. et al. 2003, Nat 423, 847
- [4] Bartos I., Brady P., Marka S. 2013, Class. Quant. Grav. 30, 123001
- [5] NASA, <http://ecuip.lib.uchicago.edu/multiwave-length-astronomy/gamma-ray/science/07.html>
- [6] Predehl P., Andritschke R., Böhringer H. et al. 2010, SPIE 7732E, 23
- [7] Khabibullin I., Sazonov S., Sunyaev R. 2012, MN 426, 1819
- [8] Amati L., Del Monte E., D'Elia V. et al. 2013, Nucl. Phys. B (in press; arXiv:1302.5276)
- [9] Gendreau K.C., Arzoumanian Z., Okajima T. 2012, SPIE 8443, 844313
- [10] Park I.H., Brandt S., Budtz-Jorgensen C. et al. 2013, NJP 15, 023031
- [11] Siellez K., Boër M., Gendre B. 2013, MN (subm.)
- [12] Aasi J., Abadie J., Abbott B.P. et al., 2013, arXiv:1304.0670
- [13] Sathyaprakash B. et al 2012, Class. Quant. Grav. 29, 124013
- [14] Abadie J., et al. 2010, Class. Quant. Grav. 27, 173001
- [15] Abbasi R., Abdou Y., Abu-Zayyad T et al. 2012, Nat. 484, 351
- [16] Whitehorn N., 2013, talk at IceCube Part. Astrophys. Symp., 2013 May 15, Madison
- [17] Hümmel S., Baerwald P., Winter W. 2012, PRL 108, 231101
- [18] Bouwens R.J., Illingworth G.D., Oesch P.A. et al. 2012, ApJ 752, L5
- [19] Tanvir N., Levan A.J., Fruchter A.S. et al. 2012, ApJ 754, 46
- [20] Johnson J.L., Greif T., Bromm V., 2008, MN 388, 26
- [21] Rossi E., Perna R., Daigne F 2008, MN 390, 675
- [22] de Souza R.S., Krone-Martins A., Ishida E.E.O., Ciardi B., 2012, A&A 545, A9
- [23] Zhu S., Racusin J., Kocevski D. et al. 2013, GCN #14471
- [24] Gilmore R.C., Bouvier A., Connaughton V. et al. 2013, Exp. Astron. 35, 413
- [25] Ghirlanda G. et al. 2013, MN (subm.)
- [26] Cucchiara A., et al. 2011, ApJ 736, C7
- [27] Tegmark M., et al. 1997, ApJ 474, 1
- [28] Yoshida N., Bromm V., Hernquist L., 2004, ApJ 605, 579
- [29] Kamada A., et al. 2013, JCAP 03, 008
- [30] Barkana R., Haiman Z., Ostriker J.P., 2001, ApJ 558, 482
- [31] Mesinger A., Perna R., Haiman Z. 2005, ApJ 623, 1
- [32] de Souza R.S., Mesinger A., Ferrara A. et al. 2013, MN (subm., arXiv:1303.5060)
- [33] Maio U., et al. 2012, MN 426, 2078
- [34] Bromm V., Yoshida N., Hernquist L., McKee C.F., 2009, Nat. 459, 49
- [35] Bromm V., Larson R.B. 2004, ARA&A 42, 79
- [36] Glover S. 2005, SSRv 117, 445
- [37] Ciardi B., Ferrara A. 2005, SSRv 116, 625
- [38] Hopkins A.M., Beacom J.F. 2006, ApJ 651, 142
- [39] Madau P., Haardt F., Rees M.J., ApJ 514, 648
- [40] Kistler M.D., Yüksel H., Hopkins A.M. 2013, arXiv:1305:1630
- [41] Abel T., Bryan G.L., Norman M.L. 2002, Sci. 295, 93
- [42] Bromm V., Coppi P.S., Larson R.B. 2002, ApJ 564, 23
- [43] Yoshida N., Omukai K., Hernquist L., Abel T. 2006, ApJ 652, 6
- [44] O'Shea B.W., Norman M.L. 2007, ApJ 654, 66
- [45] Clark P.C., Glover S., Simon C.O. et al. 2011a, Sci. 331, 1040
- [46] Greif T., Bromm V., Clark P.C. et al. 2012, MN 424, 399
- [47] Stacy A., Greif T., Klessen R.S. et al. 2013, MN 431, 1470
- [48] Turk M., Abel T., O'Shea B 2009, Sci 325, 601
- [49] Stacy A., Greif T., Bromm V. 2010, MN 403, 45
- [50] Clark P.C., Glover S., Simon C.O. et al. 2011b, ApJ 727, 110
- [51] Smith R.J., Glover S., Simon C.O. et al. 2011, MN 414, 3633
- [52] Beers T.C., Christlieb N., 2005, ARA&A 43, 531
- [53] Salvadori S., Schneider R., Ferrara A. 2007, MN 381, 647
- [54] Tumlinson J., 2007, ApJ 664, 63
- [55] Tominaga N. Umeda H., Nomoto K., 2007, ApJ 660, 516
- [56] Izutani N., Umeda H., Tominaga N. 2009, ApJ 692, 1517
- [57] Heger A., Woosley S.E. 2010 ApJ, 724, 341
- [58] Joggerst C.C. et al. 2010, ApJ 709, 11
- [59] Schneider R., Ferrara A., Salvaterra R. et al. 2003, Nat. 422, 869
- [60] Schneider R., Omukai K., Limongi M. 2012, MN 423, L60
- [61] Johnson J.L., Greif T.H., Bromm V. et al. 2009, ASP Conf. 419, p. 335
- [62] Bromm V., Loeb A., 2006, ApJ 642, 382
- [63] Campisi M.A., Maio U., Salvaterra R., Ciardi B., 2011, MN 416, 2760
- [64] Meszaros P., Rees M.J., 2010, ApJ 715, 967
- [65] Kommissarov S.S., Barkov M.V., 2010, MN 402, L25
- [66] Suwa Y., Ioka K., 2011, ApJ 726, 107
- [67] Greiner J., Krühler T., Fynbo J.P.U., et al. 2009, ApJ 693, 1610
- [68] Tanvir N.R., Fox D.B., Levan A.J. et al. 2009, Nat. 461, 1254
- [69] Salvaterra R., Della Valle M., Campana S. et al. 2009, Nat. 461, 1258
- [70] Fryer C., Woosley S.E., Hartmann D.H. 1999, ApJ 526, 152
- [71] Fynbo J.P.U., et al. 2008, ApJ 683, 321
- [72] Kistler M.D., et al. 2009, ApJ 705, L104
- [73] Elliott J., Greiner J., Khochfar S., et al. 2012, A&A 539, A113
- [74] Daigne F., Rossi E.M., Mochkovitch R. 2006, MN 372, 1034
- [75] Wanderman D., Piran T. 2010, MN 406, 1944
- [76] Ishida E.E.O., de Souza R., Ferrara A. 2011, MN 418, 500
- [77] Greiner J., et al. 2011, A&A 526, A30

- [78] Salvaterra R., Campana S., Vergani S.D. et al. 2012, *ApJ* 749, 68:
- [79] Wang F.Y., Bromm V., Greif T. et al. 2012, *ApJ* 760, 27
- [80] Schneider R., Ferrara A., Salvaterra R. et al. 2004, *MN* 351, 1379
- [81] Vreeswijk P.M., et al. 2004, *A&A* 419, 927
- [82] Black J.H., 1998, *Faraday Discuss.* 109, 257
- [83] Mao S., Mo H.J., 1998, *A&A* 339, L1
- [84] Choudhury T., Ferrara A. 2006, *MN* 371, 55
- [85] Alvarez M.A. et al., 2006, *ApJ* 639, 621
- [86] Mitra S., Choudhury T., Ferrara A. 2011, *MN* 419, 1480
- [87] Simcoe R.A. et al., 2004, *ApJ* 606, 92
- [88] Tornatore L., Ferrara A., Schneider R. 2007, *MN* 382, 945
- [89] Salvaterra R., Maio U., Ciardi B., et al. 2013, *MN* 429, 2718
- [90] Kawai N., et al. 2006, *Nat.* 440, 184
- [91] Ellis R.S., et al. 2013, *ApJ* 763, L7
- [92] Basa S., et al. 2012, *A&A* 542, A103
- [93] Savaglio S., Glazebrook K., Le Borgne D. 2009, *ApJ*, 691, 182
- [94] Bouwens R.J., et al. 2011, *ApJ* 737, 90
- [95] Noterdaeme P., Petitjean P., Carithers W.C. et al. 2012, *A&A* 547, L1
- [96] Jakobsson P., Fynbo J.P.U., Ledoux C., et al. 2006, *A&A* 460, L13
- [97] Fynbo J.P.U., Jakobsson P., Prochaska J.X., et al. 2009, *ApJS* 185, 526
- [98] Jakobsson P., Hjorth J., Malesani D., et al. 2012, *ApJ* 752, 62
- [99] Gallerani S., Ferrara A., Fan X., Choudhury T. 2008, *MN* 386, 359
- [100] Mesinger A., 2010, *MN* 407, 1328
- [101] McGeer I.D., Mesinger A., Fan X. 2011, *MN* 415, 3237
- [102] Ciardi B. et al. 2012, *MN* 423, 558
- [103] Barkana R., Loeb A., 2004, *ApJ* 601, 64
- [104] McQuinn M., et al. 2008, *MN* 388, 1101
- [105] Mesinger A. et al. 2004, *ApJ* 613, 23
- [106] Totani T., Kawai N., Kosugi G. et al. 2006, *PASJ* 58, 485
- [107] Mesinger A., Furlanetto S.R. 2008, *MN* 385, 1348
- [108] Inoue S., Salvaterra R., Choudhury T.R. et al. 2010, *MN* 404, 1938
- [109] Campana S., Thöne C.C., de Ugarte Postigo A. et al. 2010, *MN* 402, 2429
- [110] Campana S., Salvaterra R., Melandri A. et al. 2012, *MN* 421, 1697
- [111] Watson D., Jakobsson P. 2012, *ApJ* 754, 89
- [112] Behar E., et al. 2011, *ApJ* 734, 26
- [113] Starling R.L.C., Willingale R., Tanvir N.R. et al. 2013, *MN* (acc.; arXiv:1303.0844)
- [114] Nicastro F., et al. 2005, *ApJ* 629, 700
- [115] Campana S., Salvaterra R., Tagliaferri G. et al. 2011, *MN* 410, 1611
- [116] Becker J.K., 2008, *Phys. Rep.* 458, 172
- [117] Waxman E., Bahcall J. 1997, *PRL* 78, 2292
- [118] Bloom J.S. et al. 2009, *Astro2010 White paper*, arXiv:0902.1527
- [119] Phinney E.S. 2009, *Astro2010 White paper*, arXiv:0903.0098
- [120] Coward D.M., et al., 2012, *MN* 425, 2668
- [121] Klimenko S. et al., 2011, *PhRvD* 83, 102001
- [122] Dalal N. et al., 2006, *PhRvD* 74, 063006
- [123] Sathyaprakash B. et al 2010, *Class. Quant. Grav.* 27, 215006
- [124] Li L.-X., Paczyński B. 1998, *ApJ* 507, L59
- [125] Dessart L., et al. 2009, *ApJ* 690, 1681
- [126] Piran T., Nakar E., Rosswog S. 2013, *MN* 430, 2121 ack98
- [127] Sathyaprakash B.S., Schutz B.F., 2009, *Liv. Rev. Rel.* 12, No. 2
- [128] Cutler C., Thorne K.S., 2002, in: 16th GRG Conference, *World Sci. Publ.*, p. 72
- [129] Granot J. 2003, *ApJ* 596, L17
- [130] Toma K., et al. 2009, *ApJ* 698, 1042
- [131] Granot J., Königl A., 2003, *ApJ* 594, L83
- [132] Lyutikov M., Pariev V.I., Blandford R.D. 2003, *ApJ* 597, 998
- [133] Waxman E., 2003, *Nat.* 423, 388
- [134] Beloborodov A.M. 2011, *ApJ* 737, 68
- [135] Kalemci E., Boggs S. E., Kouveliotou C., et al. 2007, *ApJ Suppl.* 169, 75
- [136] McGlynn S., Clark D.J., Dean A.J. et al. 2007, *A&A* 466, 895
- [137] McGlynn S. et al., 2009, *A&A* 499, 465
- [138] Götz D., Laurent P., Lebrun F. et al. 2009, *ApJ* 695, L208
- [139] Yonetoku D. et al., 2011, *ApJ* 743, L30
- [140] Yonetoku D. et al., 2012, *ApJ* 758, L1
- [141] Götz D., Covino S. Fernandez-Soto A. et al. 2013, *MN* (in press, arXiv:1302.4186)
- [142] Fan Y.-Z., Wei D., Xu D. 2007, *MN* 376, 1857
- [143] Laurent P., Götz D., Binétruy P. et al. 2011, *Phys. Rev. D* 83, 12, 121301
- [144] Toma K. et al., 2012, *Phys. Rev. D* 109, 24
- [145] Gal-Yam A. 2012, *Sci.* 337, 927
- [146] Bloom J.S., Giannios D., Metzger B.D. et al. 201, *Sci.* 333, 203
- [147] Komossa S. 2012, *EPJ Web Conf.* 39, id. 02001
- [148] Meegan C., et al. 2009, *ApJ* 709, 791
- [149] Hudec R., Pina L., Marsikova V., et al. 2011, *AIP Conf. Proc.* 1358, p. 423
- [150] Tichy V. et al. 2011, *NIM Phys. Res. A.* 633, p. S169
- [151] Burrows D.N., Fox D., Palmer D. et al. 2012, *Mem. S.A. It.* 21, p. 59
- [152] Gehrels N., Barthelmy S.D., Cannizzo J.K., 2012, *Proc. IAU Symp.* 285, p. 41
- [153] Greiner J., Mannheim K., Aharonian F. et al. 2012, *Exp. Astr.* 34, 551
- [154] Krühler T., Schady P., Greiner J. et al. 2011, *A&A* 526, A153
- [155] den Herder J.-W., Piro L., Ohashi T. et al. 2012, *Exp. Astr.* 34, 519
- [156] Feroci M., Stella L., van der Klis M. et al. 2012, *Exp. Astr.* 34, 415